AFRL-RB-WP-TR-2009-3241

ADJOINT SENSITIVITIES OF TIME-PERIODIC NONLINEAR STRUCTURAL DYNAMICS VIA MODEL REDUCTION

Bret Stanford, Philip Beran, and Mohammad Kurdi

Design and Analysis Methods Branch
Structures Division

October 2009
Interim Report

AIR FORCE RESEARCH LABORATORY
AIR VEHICLES DIRECTORATE
WRIGHT-PATTERSON AIR FORCE BASE, OH 45433-7542
AIR FORCE MATERIEL COMMAND
UNITED STATES AIR FORCE

NOTICE AND SIGNATURE PAGE

*//Signature//

RICHARD D. SNYDER
Research Aerospace Engineer
Design and Analysis Methods Branch
Structures Division

//Signature//

DENIS P. MROZINSKI
Chief
Design and Analysis Methods Branch
Structures Division

//Signature//

JOHN A. BOWLUS
Chief
Structures Division
Air Vehicles Directorate

*Disseminated copies will show "//Signature//" stamped or typed above the signature blocks.

REPORT DOCUMENTATION PAGE

Form Approved
OMB No. 0704-0188

1. REPORT DATE *(DD-MM-YY)*	2. REPORT TYPE	3. DATES COVERED *(From - To)*
October 2009	Interim	01 December 2007 – 07 October 2009

4. TITLE AND SUBTITLE
ADJOINT SENSITIVITIES OF TIME-PERIODIC NONLINEAR STRUCTURAL DYNAMICS VIA MODEL REDUCTION

5a. CONTRACT NUMBER
In-house

5b. GRANT NUMBER

5c. PROGRAM ELEMENT NUMBER
0601102

6. AUTHOR(S)
Bret Stanford, Philip Beran, and Mohammad Kurdi

5d. PROJECT NUMBER
A0F0

5e. TASK NUMBER

5f. WORK UNIT NUMBER
0B

7. PERFORMING ORGANIZATION NAME(S) AND ADDRESS(ES)
Design and Analysis Methods Branch (AFRL/RBSD)
Structures Division
Air Force Research Laboratory, Air Vehicles Directorate
Wright-Patterson Air Force Base, OH 45433-7542
Air Force Materiel Command, United States Air Force

8. PERFORMING ORGANIZATION REPORT NUMBER
AFRL-RB-WP-TR-2009-3241

9. SPONSORING/MONITORING AGENCY NAME(S) AND ADDRESS(ES)
Air Force Research Laboratory
Air Vehicles Directorate
Wright-Patterson Air Force Base, OH 45433-7542
Air Force Materiel Command
United States Air Force

10. SPONSORING/MONITORING AGENCY ACRONYM(S)
AFRL/RBSD

11. SPONSORING/MONITORING AGENCY REPORT NUMBER(S)
AFRL-RB-WP-TR-2009-3241

12. DISTRIBUTION/AVAILABILITY STATEMENT
Approved for public release; distribution unlimited.

13. SUPPLEMENTARY NOTES
Report contains color. PAO Case Number: 88ABW 2009-2313, 29 May 2009. Report contains color.

14. ABSTRACT
This work details a comparative analysis of six methods for computing the transient system response and adjoint design derivatives of a nonlinear structure under a periodic external actuation. Time marching via implicit integration, a time-periodic spectral element method, and a time-periodic cyclic-implicit method are all considered, each with or without POD-based model reduction of the system of equations. Details of each method, and the concomitant adjoint sensitivities, are provided in terms of accuracy, stability, and Jacobian topology (sparsity). Each method is used for a gradient-based optimization of a nonlinear planar beam, periodically actuated at its root, subject to a large number of structural design parameters. The method with lowest computational design cost is found to be a strong function of the harmonic content and the nonlinearity of the transient response, as well as the size (i.e., mesh density) of the finite element system.

15. SUBJECT TERMS
adjoint, nonlinear structure, proper orthogonal decomposition, spectral element method

16. SECURITY CLASSIFICATION OF:			17. LIMITATION OF ABSTRACT:	18. NUMBER OF PAGES	19a. NAME OF RESPONSIBLE PERSON (Monitor)
a. REPORT	b. ABSTRACT	c. THIS PAGE			Richard D. Snyder
Unclassified	Unclassified	Unclassified	SAR	40	19b. TELEPHONE NUMBER *(Include Area Code)* N/A

Standard Form 298 (Rev. 8-98)
Prescribed by ANSI Std. Z39-18

TABLE OF CONTENTS

TABLE OF FIGURES

INTRODUCTION

The computational cost associated with the analysis, design, and optimization of the transient behavior of a nonlinear mechanical system can be very high. Such problems are typically solved with time marching schemes, via a temporal finite difference of the set of ordinary differential equations (which are commonly formulated with spatial finite element methods). Implicit time marching schemes are preferred for long-duration structural dynamics problems[1], which require the solution of a system of equations many times within each time step for a nonlinear system (to drive the residual to zero with, for example, a Newton-Raphson update loop[2]). Conservation of energy within each time step of an implicit scheme can be difficult to enforce under the presence of strong nonlinearities[3], potentially leading to instabilities. Periodically-actuated structures may take many cycles for the response to set up into a time-periodic state; time marching schemes can be inefficient if the transients decay slowly[4].

Finally, in the event that a large number of design parameters are of interest for system optimization, analytical sensitivities of a metric of the unsteady nonlinear response with respect to these variables must be provided to the optimization for a gradient-based search. It is well-known that for design studies with a larger number of design variables than constraints, adjoint methods are less expensive than direct methods[5]. The latter directly computes the derivative of the system response with respect to the design variables, while the former skips this (typically) superfluous quantity in favor of an adjoint vector, which is independent of the design variables. The adjoint method, however, is notoriously cumbersome for nonlinear time marching problems[6]. The differential equation for the adjoint vector is provided with terminal conditions, and must be integrated in reverse[7]: the system response and the adjoint cannot be computed simultaneously, and the storage costs can be large.

One potential solution to all of the aforementioned issues is a time-periodic scheme. These methods approximate the time derivative operators in the set of ordinary differential equations as a set of algebraic equations, which can then be solved to compute the entire time response simultaneously. Furthermore, a time-periodic condition can be enforced within the system to compute only the time-periodic response, bypassing the initial transients completely. Having solved the nonlinear algebraic system of equations for the time-periodic response, the adjoint vector (and subsequent design derivatives) are easily and inexpensively computed[8, 9]. Three general methods are commonly used for such a time-periodic analysis: harmonic balance methods, cyclic-implicit methods, and spectral element methods. The harmonic balance method involves approximating each structural degree of freedom as a Fourier series, and then solving for the coefficients associated with each harmonic[10], or recasting the problem in the time domain[11], among a variety of approaches. The cyclic-implicit method uses a time marching scheme over an actuation cycle to produce the relationship between the response at adjacent time steps, and then sets the system response at the final step identical to that at the first step[12]. Finally, the spectral element method discretizes the time domain into elements[13, 14], with a polynomial approximation of the solution within each spectral element[4].

The harmonic balance method may suffer from the global nature of the Fourier approximation in terms of computational efficiency[15] for systems with a large range of periodic

content. Furthermore, excessive nonlinearity can cause the higher harmonics to corrupt the lower harmonics (aliasing), producing non-physical solutions and non-convergence of the Fourier series[11]; the harmonic balance method will not be considered in this work. Of the two remaining methods (cyclic-implicit and spectral elements), two substantial issues are encountered upon implementation. The first is that the Jacobian of either method becomes relatively ill-conditioned as the time-periodic assumption is enforced[4], leading to convergence issues within a Newton-Raphson loop if the nonlinearities are strong. The second issue is that the size of the Jacobian can be extremely large: the product of the number of spatial and temporal degrees of freedom. The computational cost of solving this system can be drastically alleviated by projecting the system of ordinary differential equations onto a reduced basis, prior to conversion to a set of algebraic equations via either spectral elements or the cyclic-implicit method.

Many basis functions can be reasonably used, though POD modes (proper orthogonal decomposition) are the most popular for nonlinear systems, and will be used here. POD is a linear method whose bases minimize the Euclidean norm of the distance between the full order response and the reduced generalized coordinates; as such, for a given number of modes no other basis will be able to capture as much information[16]. In general, very few POD modes (relative to the number of spatial degrees of freedom) are needed for an accurate reconstruction[17], though the modes must be computed by obtaining samples (snapshots) of the full order nonlinear transient analysis. Data from the time-periodic methods ought not be used for snapshots, as these methods compute the entire response simultaneously, rendering the model reduction obsolete. Alternatively, implicit integration can be run through a training period, the POD modes can be computed to construct the reduced order model (ROM), which can then be converted into a set of algebraic system of equations for time-periodic analysis. Having done this, the reduced cyclic adjoint vector is computed for design sensitivities.

The work presents a comparative analysis of six methods for computation of system response and adjoint sensitivities of a nonlinear structure under periodic actuation: time marching implicit integration, the cyclic-implicit method, and the spectral element method, with each method considered both with and without POD-based model reduction. A brief derivation is provided for each, for both system response and adjoint sensitivity computations. The salient issues pertaining to ROM construction are provided as well. The system under consideration is a two-dimensional elastic beam periodically actuated at its base through a prescribed rotation. The computational cost of structural optimization of the beam is provided for cases with weak and strong geometric nonlinearities, with a low (i.e., sinusoidal) and high harmonic content, for each of the six methods.

NONLINEAR BEAM DYNAMICS

This work is concerned with the nonlinear deformations of a planar elastic beam, periodically actuated at its base, as seen in Figure 1. Two different coordinate systems must be used to develop the equations of motion: a floating frame which rotates with the beam (x-y), and is attached to it base, and a fixed inertial frame (X-Y). The beam is discretized into finite elements, and each node is given three degrees of freedom: axial displacement, transverse displacement, and rotation. The beam is considered to be clamped at its base, in the floating frame, and the deformations are computed in the floating frame as well. The length of the beam is 1 m, the square cross-sectional area is 4 cm^2, the density is 50 kg/m^3, and the elastic modulus is 600 MPa. The prescribed rotation is:

$$\theta(t) = \frac{\pi}{4 \cdot \sin^{-1}(K)} \cdot \sin^{-1}\left(K \cdot \sin\left(\omega \cdot t + \frac{\pi}{2}\right)\right) \tag{1}$$

The amplitude is fixed at 45º, and K lies between 0 and 1. At the lower limit, θ becomes sinusoidal, while at the upper limit θ approaches a triangular waveform[18]. For this work, K values of 0.01 and 0.99 are studied (as seen in Figure 2), with actuation frequencies (ω) of 15 and 40 rad/s (the latter of which imposes strong geometric nonlinearities upon the beam, from inertial loads).

The equations of motion for the beam are:

$$[M] \cdot \{\ddot{u}\} + [C] \cdot \{\dot{u}\} + \{P\} = \{F\} \qquad [K] = \frac{\partial\{P\}}{\partial\{u\}} \tag{2}$$

where the deformation vector {u} is as defined above (measured in the body-fixed coordinate system), [M] is a consistent mass matrix, [C] is a damping matrix composed of skew-symmetric Coriolis terms and symmetric damping terms (Rayleigh damping, given by 10·[M]), the internal force {P} is a vector of internal forces (a nonlinear function of the deformation {u}) and {F} is an external force vector due to the rigid body inertial motions. Though not explicitly included in Eq. 2, the tangent stiffness [K] is needed for a Newton-Raphson iteration scheme. Inertial portions of Eq. 2 are computed with standard multibody dynamics techniques, while elastic portions are computed with a corotational method[19]. The solution of this set of nonlinear equations of motion will provide the beam deformation {u} as a function of time.

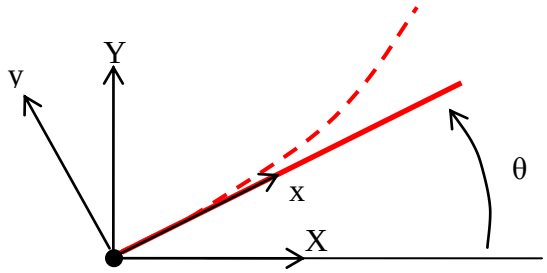

Figure 1. Planar elastic rotating beam problem description.

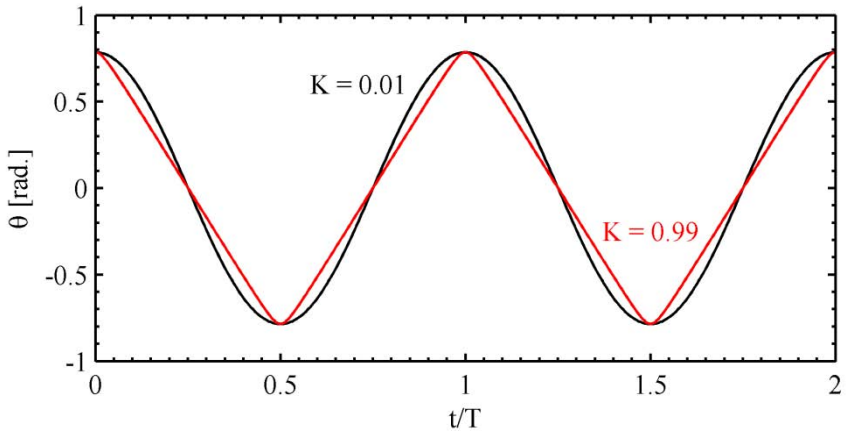

Figure 2. Actuation profiles for extreme values of K.

TIME MARCHING METHODS

An implicit Newmark method is used to integrate the equations of motion (Eq. 2) in time, while a Newton-Raphson equilibrium loop within each time step handles the structural nonlinearities. This method involves a first-order expansion of the nonlinear internal forces at consecutive time steps i and i+1 via the tangent stiffness matrix[2]:

$$\{P\}|_{i+1} = \{P\}|_i + [K]|_i \cdot \{\Delta u\} \qquad \{\Delta u\} = \{u\}|_{i+1} - \{u\}|_i \tag{3}$$

Furthermore, the velocity and acceleration terms at time step i+1 are approximated with the Newmark method[1]:

$$\{\ddot{u}\}|_{i+1} = \frac{1}{\beta \cdot \Delta t^2} \cdot (\{\Delta u\} - \Delta t \cdot \{\dot{u}\}|_i) - \left(\frac{1}{2 \cdot \beta} - 1\right) \cdot \{\ddot{u}\}|_i \tag{4}$$

$$\{\dot{u}\}|_{i+1} = \frac{\gamma}{\beta \cdot \Delta t} \cdot \{\Delta u\} - \left(\frac{\gamma}{\beta} - 1\right) \cdot \{\dot{u}\}|_i - \Delta t \cdot \left(\frac{\gamma}{2 \cdot \beta} - 1\right) \cdot \{\ddot{u}\}|_i \tag{5}$$

where γ and β are Newmark integration controls, set to 0.5 and 0.25, respectively. The three above approximations are substituted into Eq. 2, and the equations of motion at time step i+1 then become:

$$\begin{aligned} \left(\frac{1}{\beta \cdot \Delta t^2} \cdot [M] + \frac{\gamma}{\beta \cdot \Delta t} \cdot [C]|_{i+1} + [K]|_i\right) \cdot \{\Delta u\} \; &= \{F\}|_{i+1} - \{P\}|_i \\ + [M] \cdot \left(\frac{1}{\beta \cdot \Delta t} \cdot \{\dot{u}\}|_i + \left(\frac{1}{2 \cdot \beta} - 1\right) \cdot \{\ddot{u}\}|_i\right) \; &+ [C]|_{i+1} \\ \cdot \left(\left(\frac{\gamma}{\beta} - 1\right) \cdot \{\dot{u}\}|_i + \Delta t \cdot \left(\frac{\gamma}{2 \cdot \beta} - 1\right) \cdot \{\ddot{u}\}|_i\right) & \end{aligned} \tag{6}$$

where [M] is constant, and has no time step subscript. Newton-Raphson equilibrium iterations within each time step are undertaken by conditionally updating the solution $\{u\}|_{i+1}$, computing the velocity and acceleration, and then computing the residual at time step i+1:

$$\{R\}|_{i+1} = \{F\}|_{i+1} - \{P\}|_{i+1} - [M] \cdot \{\ddot{u}\}|_{i+1} - [C]|_{i+1} \cdot \{\dot{u}\}|_{i+1} \tag{7}$$

This residual is then added to the external force vector $\{F\}|_{i+1}$, $\{\Delta u\}$ is recomputed, and the process repeats until the residual is driven to zero.

Having solved the system of equations, it is assumed here that an objective function will take the form of a scalar quantity, integrated in time[20]:

$$g = \int_0^{t_f} G(t) \cdot H(t - t_o) \cdot dt \tag{8}$$

where G is a time-dependent property of the beam deformation (displacement, stresses, vibration frequency, etc.), and H is the Heaviside step function. Thus, it is only desirable to optimize the beam's performance over a single actuation period, once the motion has become time-periodic, between t_o and t_f. For reasons that will be discussed below, it is still necessary to define the integral from 0 to t_f, even though information prior to t_o is of no interest. The derivative of the objective function with respect to an unspecified vector of design variables, $\{x\}$, is:

$$\frac{\partial g}{\partial \{x\}} = \int_0^{t_f} \frac{\partial G}{\partial \{u\}}^T \cdot \frac{\partial \{u\}}{\partial \{x\}} \cdot H(t - t_o) \cdot dt \tag{9}$$

where $\{u\}$ is the solution of the nonlinear system of equations. Computation of this derivative is facilitated by taking the derivative of Eq. 2:

$$\frac{\partial [M]}{\partial \{x\}} \cdot \{\ddot{u}\} + [M] \cdot \frac{\partial \{\ddot{u}\}}{\partial \{x\}} + \frac{\partial [C]}{\partial \{x\}} \cdot \{\dot{u}\} + [C] \cdot \frac{\partial \{\dot{u}\}}{\partial \{x\}} + [K] \cdot \frac{\partial \{u\}}{\partial \{x\}} + \frac{\partial \{P\}}{\partial \{x\}} = \frac{\partial \{F\}}{\partial \{x\}} \tag{10}$$

The adjoint method is undertaken by pre-multiplying the equations of motion by an adjoint vector $\{\lambda\}$, and adding this term to the derivative of the objective function[7]:

$$\frac{\partial g}{\partial \{x\}} = \int_0^{t_f} \left(\frac{\partial G}{\partial \{u\}}^T \cdot \frac{\partial \{u\}}{\partial \{x\}} \cdot H(t - t_o) + \{\lambda\}^T \cdot \left(\begin{matrix} \frac{\partial [M]}{\partial \{x\}} \cdot \{\ddot{u}\} + [M] \cdot \frac{\partial \{\ddot{u}\}}{\partial \{x\}} + \frac{\partial [C]}{\partial \{x\}} \cdot \{\dot{u}\} + \\ [C] \cdot \frac{\partial \{\dot{u}\}}{\partial \{x\}} + [K] \cdot \frac{\partial \{u\}}{\partial \{x\}} + \frac{\partial \{P\}}{\partial \{x\}} - \frac{\partial \{F\}}{\partial \{x\}} \end{matrix} \right) \right) \cdot dt \tag{11}$$

Integration by parts is used (twice) to remove the time derivative terms within the response derivatives:

$$\frac{\partial g}{\partial \{x\}} = \int_0^{t_f} \left(\begin{matrix} \{\lambda\}^T \cdot \left(\frac{\partial [M]}{\partial \{x\}} \cdot \{\ddot{u}\} + \frac{\partial [C]}{\partial \{x\}} \cdot \{\dot{u}\} + \frac{\partial \{P\}}{\partial \{x\}} - \frac{\partial \{F\}}{\partial \{x\}} \right) + \\ \left(\frac{\partial G}{\partial \{u\}}^T \cdot H(t - t_o) + \{\ddot{\lambda}\}^T \cdot [M] - \{\dot{\lambda}\}^T \cdot [C] + \{\lambda\}^T \cdot ([K] - [\dot{C}]) \right) \cdot \frac{\partial \{u\}}{\partial \{x\}} \end{matrix} \right) \cdot dt \tag{12}$$

$$+\{\lambda\}^T \cdot [C] \cdot \frac{\partial \{u\}}{\partial \{x\}}\Big|_0^{t_f} + \{\lambda\}^T \cdot [M_r] \cdot \frac{\partial \{\dot{u}\}}{\partial \{x\}}\Big|_0^{t_f} - \{\dot{\lambda}\}^T \cdot [M] \cdot \frac{\partial \{u\}}{\partial \{x\}}\Big|_0^{t_f}$$

This equation would suggest the following boundary conditions:

$$\frac{\partial \{u\}}{\partial \{x\}}\Big|_{t=0} = \frac{\partial \{\dot{u}\}}{\partial \{x\}}\Big|_{t=0} = 0 \qquad \{\lambda\}|_{t=t_f} = \{\dot{\lambda}\}|_{t=t_f} = 0 \tag{13}$$

The first two conditions are satisfied due to the fact that initial conditions upon the beam's dynamics are prescribed (both position and velocity are zero at the initial condition). If the integration bounds were taken from t_o to t_f, rather than starting at zero, this would no longer be true. As the very purpose of the adjoint method is to entirely skip the generally unneeded

derivatives of the system response ($\partial\{u\}/\partial\{x\}$), a direct method (which does compute these terms) would have to be marched from t = 0 to t_o in order to compute these derivatives, and then the adjoint method could be undertaken from t_o to t_f[7]. From a computational cost perspective, it makes more sense to integrate from 0 to t_f, and use a Heaviside step function. The latter two relations represent terminal conditions on the adjoint vector. This vector can now be solved for with:

$$\{\ddot{\lambda}\}^T \cdot [M] - \{\dot{\lambda}\}^T \cdot [C] + \{\lambda\}^T \cdot \left([K] - [\dot{C}]\right) = -\frac{\partial G}{\partial \{u\}}^T \cdot H(t - t_o) \tag{14}$$

As intended, this adjoint vector is independent of the design variables, and must be computed by integrating backwards in time with an implicit Newmark method, starting with the terminal conditions and working backwards to the initial conditions. Thus, the response **{**u**}** and the adjoint vector {λ**}** cannot be computed simultaneously. The system matrices (mass, damping, and tangential stiffness) at each time step then must either be stored during the forward integration for future adjoint computations (impractical for large problems), or recomputed during the reverse integration. Having computed the reduced adjoint vector, the sought-after design sensitivity is given by:

$$\frac{\partial g}{\partial \{x\}} = \int_0^{t_f} \{\lambda\}^T \cdot \left(\frac{\partial [M]}{\partial \{x\}} \cdot \{\ddot{u}\} + \frac{\partial [C]}{\partial \{x\}} \cdot \{\dot{u}\} + \frac{\partial \{P\}}{\partial \{x\}} - \frac{\partial \{F\}}{\partial \{x\}}\right) \cdot dt \tag{15}$$

MODEL REDUCTION

As noted above, the computational cost associated with design optimization via implicit integration is large, particularly for structures with a large number of degrees of freedom (N_{DOF}): each equilibrium iteration within each time step requires the solution to a set of equations (Eq. 6). Furthermore, the time step must be kept relatively small. This is not necessarily due to stability concerns (the implicit method is guaranteed stable for linear systems, though nonlinearities may lead to instabilities[3]), but due to limited range of convergence of the Newton-Raphson algorithm: the initial guess at time step i is the converged solution at step i-1. Finally, the computation of the adjoint vector (Eq. 14) can be cumbersome, as the terms must be reestablished during the reverse integration. These problems can all be attenuated, to some degree, with reduced order modeling, wherein the system of equations is projected onto a reduced basis. This is done by approximating the structural response as a linear combination of basis vectors:

$$u(t) = \sum_{i=1}^{N_r} \eta_i(t) \cdot \phi_i \qquad \{u\} = [\Phi] \cdot \{\eta\} \tag{16}$$

where $\{u\}$ has been reduced to a set of generalized coordinates $\{\eta\}$ through a matrix of basis vectors, or modes: $[\Phi]$. The number of modes needed (N_r) is typically much less than the size of the original system (N_{DOF}). The reduced basis is constructed with POD modes, which requires computing the response of the full order model (FOM, essentially Eq. 2), and storing the results at several time steps[16] in a snapshot matrix:

$$[S] = \left[\{u\}|_1 \quad \{u\}|_2 \quad \cdots \quad \{u\}|_{N_{steps}}\right]^T \tag{17}$$

where $[S]$ is an N_{steps} x N_{DOF} matrix. The following eigenproblem must then be solved[16]:

$$[S]^T \cdot [S] \cdot [V] = [V] \cdot [\Lambda] \tag{18}$$

The eigenvectors of the system are contained in the matrix $[V]$, and the eigenvalues are given in the diagonal matrix $[\Lambda]$. The reduced basis is then computed as:

$$[\Phi] = [S] \cdot [V] \tag{19}$$

Upon solution of this eigenvalue problem, a large number of basis functions are available, but a relatively small number (N_r) can be utilized in practice. A suitable retention number can be inferred from the relative size of the eigenvalues $[\Lambda]$, which provide the system energy captured by each mode.

The nonlinear system of equations (Eq. 2) can be projected into this reduced space by introducing the approximate form of the beam deformation (Eq. 16), and pre-multiplying through by the modal matrix:

$$[\Phi]^T \cdot [M] \cdot [\Phi] \cdot \{\ddot{\eta}\} + [\Phi]^T \cdot [C] \cdot [\Phi] \cdot \{\dot{\eta}\} + [\Phi]^T \cdot \{P\} = [\Phi]^T \cdot \{F\} \tag{20}$$

$$[M_r] \cdot \{\ddot{\eta}\} + [C_r] \cdot \{\dot{\eta}\} + \{P_r\} = \{F_r\} \tag{21}$$

where the subscript (r) implies a reduced term. The reduced parameters (force vectors and stiffness, damping, and mass matrices) can then be used with the above Newmark integration scheme to compute $\{\eta\}$ at each time step. The method given in Eq. 20 requires that the finite element terms be computed in the full order space, assembled, and then reduced with pre- and post-multiplication. A superior method, used here, is to perform reduction on an element-by-element basis, rather than for the entire system[17]. For example:

$$[K_r] = \sum_{e=1}^{E} [\Phi_e]^T \cdot [K_e] \cdot [\Phi_e] \tag{22}$$

where the global matrix is found through a typical assembly process of each finite element (e). $[\Phi_e]$ refers to the modal matrix terms corresponding to the degrees of freedom found in the e^{th} finite element, and is a subset of $[\Phi]$.

Using the reduced order model alleviates computational cost through storage and system solver requirements (as each reduced term is of the small size N_r x N_r, albeit full). The reduced storage cost also has significant ramifications for adjoint sensitivities, as discussed below. Model reduction incurs three cost penalties, however. First, the solution of the POD eigenproblem (Eq. 18) can be costly for a large number of time steps; second, the assembly of the global finite element matrices (Eq. 22) requires more operations in the reduced space due to the pre- and post-multiplication of the modal matrix; third (and typically the most severe), the snapshot matrix must be populated with data from the full order model.

The following method is used to compute the basis functions. Using implicit integration, the full order model is integrated from t = 0 to a specified t_{FOM}. The results at each time step are stored within the snapshot matrix (Eq. 17), which is used to compute the POD modes (Eq. 19). These modes can be used to reduce the equations of motion, re-integrated from t = 0 to the last

time step of interest (typically after the solution becomes time-periodic), or they can be used with the time-periodic methods described below. The training period, t_{FOM}, is an important metric: if the value is too small, the snapshot matrix will not adequately capture the important dynamical characteristics of the system. If the value is too large, the cost penalties associated with running the full order model will be severe. This trade-off is clearly demonstrated below.

The sensitivities of the ROM are found in a similar manner to above, with the reduced adjoint vector given as:

$$\begin{gathered}\left\{\ddot{\lambda}_r\right\}^T \cdot [M_r] - \left\{\dot{\lambda}_r\right\}^T \cdot [C_r] + \{\lambda_r\}^T \cdot \left([K_r] - [\dot{C}_r]\right) = -[\Phi]^T \cdot \frac{\partial G}{\partial \{u\}}^T \cdot H(t - t_o) \\ \{\lambda_r\}|_{t=t_f} = \left\{\dot{\lambda}_r\right\}\Big|_{t=t_f} = 0\end{gathered} \tag{23}$$

It should be noted that, unlike in the full order model, where all of the system matrices and vectors must be re-established during the reverse integration, now all of the terms are small enough to be stored in memory during the forward integration. As such, the computational cost associated with the reduced adjoint vector is very small. It is also assumed here that the reduced basis (POD modes) is not a function of the design variables, which is obviously untrue. It has been shown that in using reduction of linear structural dynamics to modal coordinates for sensitivity analysis, the derivative of the linear eigenvectors with respect to the design parameters is negligible[8]. A similar assumption with the POD modes will be shown below to be acceptable. Having computed the reduced adjoint vector, the sought-after design sensitivity is given by:

$$\frac{\partial g}{\partial \{x\}} = \int_0^{t_f} \{\lambda_r\}^T \cdot \left(\frac{\partial [M_r]}{\partial \{x\}} \cdot \{\ddot{\eta}\} + \frac{\partial [C_r]}{\partial \{x\}} \cdot \{\dot{\eta}\} + \frac{\partial \{P_r\}}{\partial \{x\}} - \frac{\partial \{F_r\}}{\partial \{x\}}\right) \cdot dt \tag{24}$$

Results pertaining to ROM accuracy, for both the system response and the adjoint computations, are given in Figure 3, for an objective function g of:

$$g = \int_0^{t_f} \left(\delta_{tip}\right)^2 \cdot H(t - t_o) \cdot dt \tag{25}$$

where δ_{tip} is the transverse displacement of the beam's tip, measured in the floating frame of Figure 1. Minimizing this metric will essentially decrease the beam deformation throughout the actuation cycle (though only the deformation during the final, time-periodic motion is considered in computing the objective function). The normalized tip displacement is given as a function of time in the upper plot of Figure 3, for the full order model (integration of Eq. 2) and reduced

order models with a varying number of retained POD modes (integration of Eq. 21). For an actuation frequency of 40 rad/s and K set to 0.01, the response is relatively nonlinear (approaching 50% of the beam length) and smooth. The initial transients decay after 9 actuation cycles, leaving a cyclic sinusoidal response in phase with the rotation actuation. The reduced order models are computed by integrating the full order model through a training period of half of an actuation cycle, with the data at each time step used for the snapshot matrix. A ROM with 2 modes is inaccurate, diverging from the correct response shortly after the training period, 4 modes has minor inaccuracies but largely captures the time-periodic response, and 6 modes is very accurate for both the initial transients and time-periodic response.

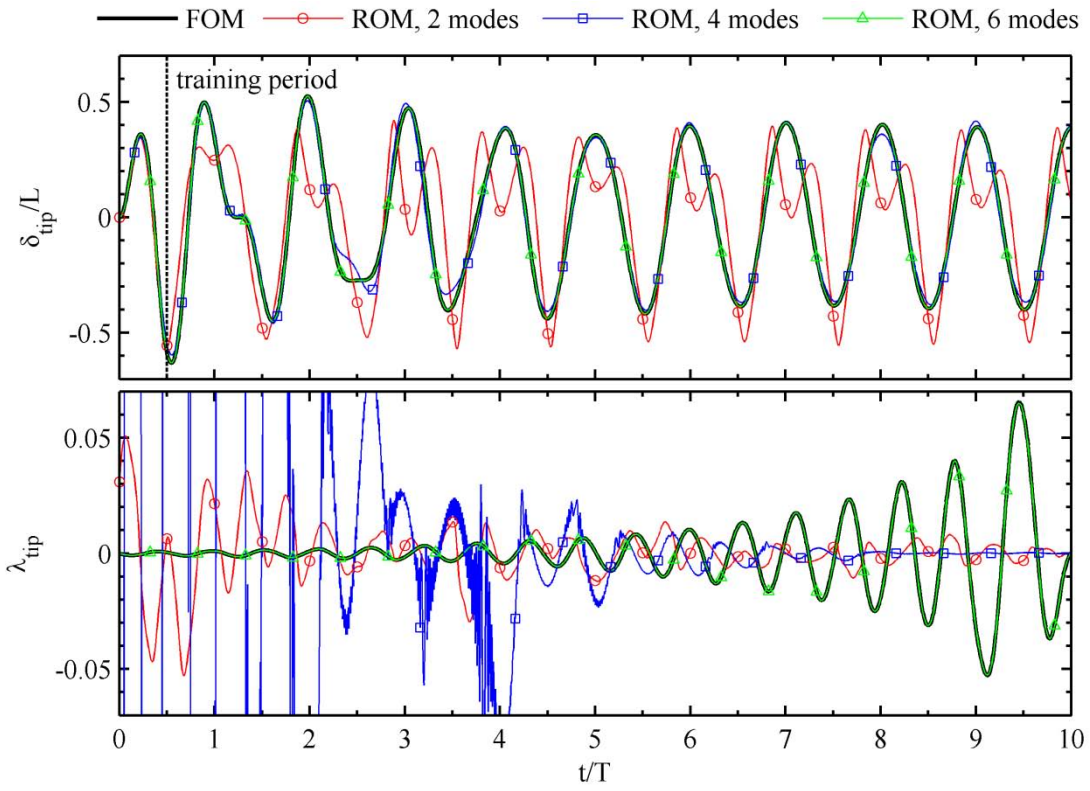

Figure 3. System response and adjoint accuracy for various reduced order models: ω = 40 rad/s, K = 0.01.

Using either Eq. 14 or Eq. 23, the adjoint vector can be computed (which is only effected by the objective function of Eq. 25, not the as-yet unspecified design variables). For both cases, the adjoint vector is analogous to the system response due to an oscillating transverse point load at the tip (equal to $-2\cdot \delta_{tip}$) which only operates within the last actuation cycle of motion. The member of the adjoint vector that corresponds to the δ_{tip} structural degree of freedom is given in the lower plot of Figure 3. For the implicit integration, the adjoint has zero terminal conditions (Eq. 13), and is integrated backwards in time according to Eq. 14. The "dummy load"[8] actuates the system within the final actuation cycle, and is then removed (as the objective function in Eq. 20 is only concerned with the final time-periodic response). Moving backwards from $9\cdot T$ to 0,

the adjoints resemble a damped free vibration (albeit with a negative damping matrix, Eq. 14), which decays to zero as t approaches 0. For the reduced adjoint vector, a ROM with 2 modes is expectedly inaccurate, though increasing the number of modes to 4 leads to instabilities in the adjoint integration. A ROM with 6 modes is needed for a stable and accurate adjoint computation.

The logarithmic error in the objective function and the norm of the design sensitivity (Eq. 24, where the design variables are the cross-sectional area of each beam element) is given in Figure 4, where the error is defined as the difference between the full and reduced order models. Along with the data of Figure 3, it can be seen that more modes are generally needed for an accurate sensitivity analysis than for the system response. From the left side of Figure 4, there is an accuracy trade-off between the number of modes needed and the duration of the training period. If the training period is too short however (0.1·T, for the example given), increasing the number of modes does not improve the accuracy. It can further be seen from the right side of Figure 4 that the number of modes needed for an accurate ROM is a weak function of the number of structural degrees of freedom[17], which should ease the computational cost during the time integration. The cost of solving the full order system is expected to be, in a best-case scenario, $O(N_{DOF})$ for each iteration, if a sparse solver is employed. The cost of solving the reduced order system is, conservatively, $O(N_r^3)$, as the reduced matrices are all full. Computational cost savings are realized if N_{DOF} grows much faster than N_r^3, as indicated by Figure 4.

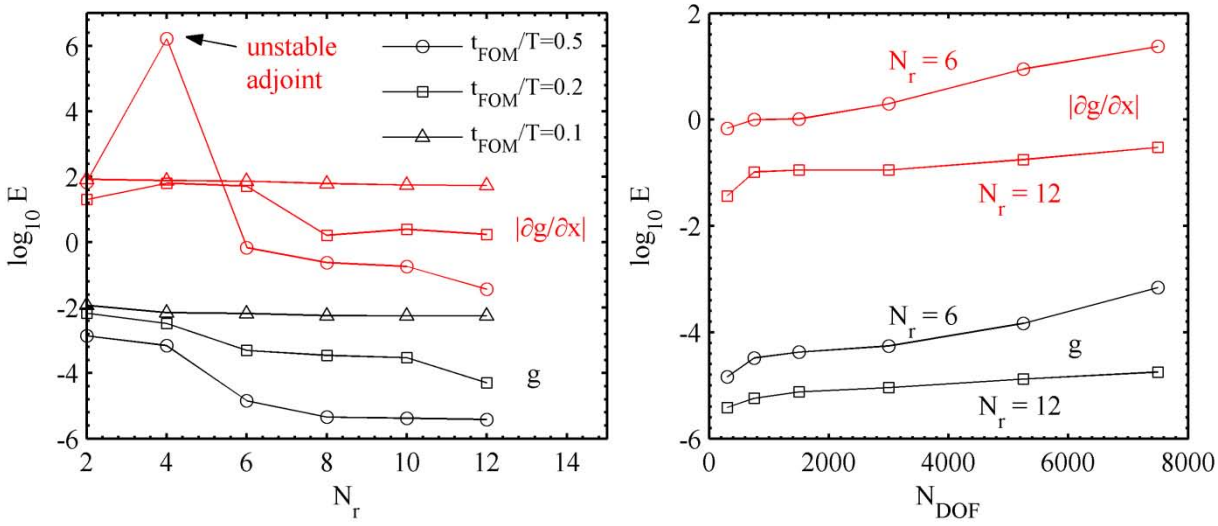

Figure 4. ROM accuracy as a function of the number of modes (left, with NDOF fixed at 30), or the number of structural degrees of freedom (right): ω = 40 rad/s, K = 0.01.

CYCLIC-IMPLICIT METHOD

The cyclic-implicit method uses an implicit time marching scheme over a single actuation cycle to produce the relationship between the system responses at adjacent time steps, and then sets the system response at the final step to be identical to that at the first step[12]. This is done by converting Eq. 2 into first order form, and using a Crank-Nicolson scheme to compute the system response at one time step in terms of the response at the previous step[1]:

$$\begin{aligned}\left(\frac{1}{\Delta t}\cdot\begin{bmatrix}[I] & [0]\\ [0] & [M]\end{bmatrix}+\beta\cdot\begin{bmatrix}[0] & -[I]\\ [0] & [C]\end{bmatrix}\right)\cdot\left.\begin{Bmatrix}\{u\}\\ \{\dot{u}\}\end{Bmatrix}\right|_{i+1}\\ +\left(\frac{-1}{\Delta t}\cdot\begin{bmatrix}[I] & [0]\\ [0] & [M]\end{bmatrix}+(1-\beta)\cdot\begin{bmatrix}[0] & -[I]\\ [0] & [C]\end{bmatrix}\right)\cdot\left.\begin{Bmatrix}\{u\}\\ \{\dot{u}\}\end{Bmatrix}\right|_{i}+\beta\cdot\left.\begin{Bmatrix}\{0\}\\ \{P\}\end{Bmatrix}\right|_{i+1}\\ +(1-\beta)\cdot\left.\begin{Bmatrix}\{0\}\\ \{P\}\end{Bmatrix}\right|_{i}=\beta\cdot\left.\begin{Bmatrix}\{0\}\\ \{F\}\end{Bmatrix}\right|_{i+1}+(1-\beta)\cdot\left.\begin{Bmatrix}\{0\}\\ \{F\}\end{Bmatrix}\right|_{i}\end{aligned} \tag{26}$$

$$\begin{aligned}[A]\cdot\{q\}|_{i+1}+[B]\cdot\{q\}|_{i}+\beta\cdot\{R_{int}\}|_{i+1}+(1-\beta)\cdot\{R_{int}\}|_{i}\\ =\beta\cdot\{R_{ext}\}|_{i+1}+(1-\beta)\cdot\{R_{ext}\}|_{i}\end{aligned} \tag{27}$$

where β is an integration parameter (set to 0.5 for a Crank-Nicolson scheme), and $\{q\}$, $\{R_{int}\}$, and $\{R_{ext}\}$ are generalized coordinates and forces for the first order system. Dividing an actuation cycle into N_{cyc} time steps, and further assuming that the solution state at the first time step and the final time step are identical (for time-periodicity), the following system of equations are obtained:

$$\begin{aligned}\begin{bmatrix}[A] & & & [B]\\ [B] & [A] & & \\ & [B] & \ddots & \\ & & \ddots & [A]\\ & & [B] & [A]\end{bmatrix}\cdot\begin{Bmatrix}\{q\}|_1\\ \{q\}|_2\\ \{q\}|_3\\ \vdots\\ \{q\}|_{N_{cyc}}\end{Bmatrix}\\ +\begin{Bmatrix}\beta\cdot\{R_{int}\}|_1+(1-\beta)\cdot\{R_{int}\}|_{N_{cyc}}\\ \beta\cdot\{R_{int}\}|_2+(1-\beta)\cdot\{R_{int}\}|_1\\ \beta\cdot\{R_{int}\}|_3+(1-\beta)\cdot\{R_{int}\}|_2\\ \vdots\\ \beta\cdot\{R_{int}\}|_{N_{cyc}}+(1-\beta)\cdot\{R_{int}\}|_{N_{cyc}-1}\end{Bmatrix}\\ =\begin{Bmatrix}\beta\cdot\{R_{ext}\}|_1+(1-\beta)\cdot\{R_{ext}\}|_{N_{cyc}}\\ \beta\cdot\{R_{ext}\}|_2+(1-\beta)\cdot\{R_{ext}\}|_1\\ \beta\cdot\{R_{ext}\}|_3+(1-\beta)\cdot\{R_{ext}\}|_2\\ \vdots\\ \beta\cdot\{R_{ext}\}|_{N_{cyc}}+(1-\beta)\cdot\{R_{ext}\}|_{N_{cyc}-1}\end{Bmatrix}\end{aligned} \tag{28}$$

This equation can be re-written as:

$$\left[M_{cyc}\right] \cdot \left\{U_{cyc}\right\} + \left\{P_{cyc}\right\} = \left\{F_{cyc}\right\} \qquad \left[K_{cyc}\right] = \frac{\partial \left\{P_{cyc}\right\}}{\partial \left\{U_{cyc}\right\}} \tag{29}$$

Where $\{U_{cyc}\}$, $\{P_{cyc}\}$, and $\{F_{cyc}\}$ are displacements/velocities and forces grouped by common temporal degree of freedom, for each time step in the cycle. Solution of this nonlinear system is facilitated with a nonlinear Jacobian matrix and a residual vector:

$$\left[J_{cyc}\right] = \left[M_{cyc}\right] + \left[K_{cyc}\right] \tag{30}$$

$$\left\{R_{cyc}\right\} = \left[M_{cyc}\right] \cdot \left\{U_{cyc}\right\} + \left\{P_{cyc}\right\} - \mu \cdot \left\{F_{cyc}\right\} \tag{31}$$

The system can be solved with a Newton-Raphson equilibrium loop, gradually increasing μ (load scaling factor) from 0 to 1 to ensure convergence of the solution. The solution guess at the n^{th} iteration is:

$$\left\{U_{cyc}\right\}^{n} = \left\{U_{cyc}\right\}^{n-1} - \left[J_{cyc}\right]^{-1} \cdot \left\{R_{cyc}\right\} \tag{32}$$

This process is repeated until the residual vector vanishes, at which point convergence has been obtained.

For the cyclic-implicit method, the time-integrated objective function is defined with a numerical integration:

$$g_{cyc} = \{\omega\}^{T} \cdot \left\{G_{cyc}\right\} \qquad \left\{G_{cyc}\right\} = \left\{G|_{1} \quad G|_{2} \quad \cdots \quad G|_{N_{cyc}}\right\}^{T} \tag{33}$$

where $\{\omega\}$ is a vector of integration weights. Adjoints are computed by first differentiating the objective function:

$$\frac{\partial g_{cyc}}{\partial \{x\}} = \frac{\partial g_{cyc}}{\partial \left\{U_{cyc}\right\}}^{T} \cdot \frac{\partial \left\{U_{cyc}\right\}}{\partial \{x\}} = \{\omega\}^{T} \cdot \frac{\partial \left\{G_{cyc}\right\}}{\partial \left\{U_{cyc}\right\}} \cdot \frac{\partial \left\{U_{cyc}\right\}}{\partial \{x\}} \tag{34}$$

The derivative of the system of equations (Eq. 29) is:

$$\frac{\partial\left[\mathrm{M}_{\mathrm{cyc}}\right]}{\partial\{\mathrm{x}\}}\cdot\left\{\mathrm{U}_{\mathrm{cyc}}\right\}+\left[\mathrm{J}_{\mathrm{cyc}}\right]\cdot\frac{\partial\left\{\mathrm{U}_{\mathrm{cyc}}\right\}}{\partial\{\mathrm{x}\}}+\frac{\partial\left\{\mathrm{P}_{\mathrm{cyc}}\right\}}{\partial\{\mathrm{x}\}}-\frac{\partial\left\{\mathrm{F}_{\mathrm{cyc}}\right\}}{\partial\{\mathrm{x}\}}=0 \tag{35}$$

As above, this equation is pre-multiplied by an adjoint vector, and added to the derivative of the objective function:

$$\begin{aligned}\frac{\partial \mathrm{g}_{\mathrm{cyc}}}{\partial\{\mathrm{x}\}}=\{\omega\}^{\mathrm{T}}\cdot\frac{\partial\left\{\mathrm{G}_{\mathrm{cyc}}\right\}}{\partial\left\{\mathrm{U}_{\mathrm{cyc}}\right\}}\cdot\frac{\partial\left\{\mathrm{U}_{\mathrm{cyc}}\right\}}{\partial\{\mathrm{x}\}}+\left\{\lambda_{\mathrm{cyc}}\right\}^{\mathrm{T}}\\ \cdot\left(\frac{\partial\left[\mathrm{M}_{\mathrm{cyc}}\right]}{\partial\{\mathrm{x}\}}\cdot\left\{\mathrm{U}_{\mathrm{cyc}}\right\}+\left[\mathrm{J}_{\mathrm{cyc}}\right]\cdot\frac{\partial\left\{\mathrm{U}_{\mathrm{cyc}}\right\}}{\partial\{\mathrm{x}\}}+\frac{\partial\left\{\mathrm{P}_{\mathrm{cyc}}\right\}}{\partial\{\mathrm{x}\}}-\frac{\partial\left\{\mathrm{F}_{\mathrm{cyc}}\right\}}{\partial\{\mathrm{x}\}}\right)\end{aligned} \tag{36}$$

This system of equations for the solution of the adjoint vector then becomes simply:

$$\left\{\lambda_{\mathrm{cyc}}\right\}^{\mathrm{T}}\cdot\left[\mathrm{J}_{\mathrm{cyc}}\right]=-\{\omega\}^{\mathrm{T}}\cdot\frac{\partial\left\{\mathrm{G}_{\mathrm{cyc}}\right\}}{\partial\left\{\mathrm{U}_{\mathrm{cyc}}\right\}} \tag{37}$$

Finally, the sought-after design sensitivities are given by:

$$\left\{\frac{\partial \mathrm{g}_{\mathrm{cyc}}}{\partial \mathrm{x}}\right\}=\left\{\lambda_{\mathrm{cyc}}\right\}^{\mathrm{T}}\cdot\left(\frac{\partial\left[\mathrm{M}_{\mathrm{cyc}}\right]}{\partial\{\mathrm{x}\}}\cdot\left\{\mathrm{U}_{\mathrm{cyc}}\right\}+\frac{\partial\left\{\mathrm{P}_{\mathrm{cyc}}\right\}}{\partial\{\mathrm{x}\}}-\frac{\partial\left\{\mathrm{F}_{\mathrm{cyc}}\right\}}{\partial\{\mathrm{x}\}}\right) \tag{38}$$

The cyclic-implicit method can be used in either the full or the reduced order space, by converting either Eq. 2 or Eq. 21 into the first order form of Eq. 27. In the event that the ROM is to be used, time marching of the full order model must be run through the training period to compute the POD modes, as discussed above.

SPECTRAL ELEMENT METHOD

The spectral element method is a monolithic time approximation, best described by first considering a nonlinear system with a single degree of freedom, u. The spectral element method discretizes the time domain into a finite number of elements. The width of the j^{th} spectral element (in seconds) is h^j. Each spectral element is transformed onto the interval $\zeta \in [-1, 1]$, and the solution of the dependent variable within the element is approximated by an m^{th}-order Lagrange polynomial[21]:

$$\hat{u}^j = \sum_{k=0}^{m} u^j(\zeta_k) \cdot \psi_k^j(\zeta) \tag{39}$$

where $\hat{u}^j$ is the approximate solution, $u^j(\zeta_k)$ is the solution (unknown nodal degrees of freedom in time) sampled at m locations through the element (ζ_k are the m-1 zeros of the Lobatto polynomials, as well as -1 and 1), and $\psi_k{}^j$ is the k^{th} Lagrange polynomial within spectral element j. A non-dimensional, second-order, single-degree-of-freedom system is defined within the j^{th} spectral element by:

$$\frac{4 \cdot M}{(h^j)^2} \cdot \frac{d^2 u^j}{d\zeta^2} + \frac{2 \cdot C}{h^j} \cdot \frac{du^j}{d\zeta} + p^j(\zeta) = f^j(\zeta) \tag{40}$$

where, as above, M is the mass, C the damping, p is the internal force (a nonlinear function of u), and f is the external force. The approximate solution given above can be substituted into this equation, and the residual is minimized with the Bubnov-Galerkin method[4]. The k^{th}-order Lagrange polynomial is used as a trial function:

$$\int_{-1}^{1} \psi_k^j \cdot \left(\frac{2 \cdot M}{h^j} \cdot \frac{d^2 \hat{u}^j}{d\zeta^2} + C \cdot \frac{d\hat{u}^j}{d\zeta} + \frac{h^j}{2} \cdot \left(p^j(\zeta) - f^j(\zeta) \right) \right) \cdot d\zeta = 0 \tag{41}$$

Integration by parts (twice) transfers the time derivatives from the approximate solution to the trial function:

$$\left(\frac{2 \cdot M}{h^j} \cdot \left(\psi_k^j \cdot \frac{d\hat{u}^j}{d\zeta} - \frac{d\psi_k^j}{d\zeta} \cdot \hat{u}^j \right) + C \cdot \psi_k^j \cdot \hat{u}^j \right) \Bigg|_{-1}^{1} + \tag{42}$$

$$\int_{-1}^{1}\left(\hat{u}^j\cdot\left(\frac{2\cdot M}{h^j}\cdot\frac{d^2\psi_k^j}{d\zeta^2}-C\cdot\frac{d\psi_k^j}{d\zeta}\right)+\frac{h^j}{2}\cdot\left(p^j-f^j\right)\right)\cdot d\zeta=0$$

The approximate solution can be expanded in terms of the nodal degrees of freedom at the m Lobatto points (Eq. 39), m trial functions are considered, and the integral terms are approximated with a quadrature rule:

$$\int_{-1}^{1}S(\zeta)\cdot d\zeta=\sum_{k=0}^{m}S(\zeta_k)\cdot\omega_k \tag{43}$$

where S is any function of ζ, and ω_k is the Gaussian quadrature weight at Lobatto point k. The equation of motion is now given by the following system of equations within the j^{th} spectral element:

$$M\cdot\left[\Psi_m^j\right]\cdot\left\{u_{se}^j\right\}+C\cdot\left[\Psi_c^j\right]\cdot\left\{u_{se}^j\right\}+\left[I_\omega^j\right]\cdot\left\{p_{se}^j\right\}=\left[I_\omega^j\right]\cdot\left\{f_{se}^j\right\} \tag{44}$$

Where $[\Psi_m]$ and $[\Psi_c]$ are matrices of 2^{nd} and 1^{st} derivatives of the Lagrange polynomials evaluated at the Lobatto points, and $[I_\omega]$ is a diagonal matrix containing the Lobatto weights. Explicit formulations are provided in Ref. 22. The vectors in Eq. 44 are a collocation of terms at each node within the j^{th} spectral element.

The solution over the entire domain can be obtained with a typical assembly process of the spectral elements, adding contributions to shared nodes (namely the solution at $\zeta = \pm 1$ within each element) into the same location within the global matrices. Furthermore, time-periodic solutions can be obtained by assuming that ζ_o of the first element and ζ_m of the last element are the same node. Contributions within the global matrices pertaining to this last node are added to the contributions pertaining to the first node[4]. The size of the assembled system is thus reduced from $(m \times N_{el}) + 1$ to $m \times N_{el}$, where N_{el} is the number of spectral elements, and m is the order of the approximation made within each element. For cases with more than one structural degree of freedom, the final system of equations can be computed as:

$$\begin{aligned}&\left([M]\otimes[\Psi_m]+[C]\otimes[\Psi_c]\right)\cdot\{U_{se}\}+[I]\otimes[I_\omega]\cdot\{P_{se}\}\\&\qquad=[I]\otimes[I_\omega]\cdot\{F_{se}\}\qquad[K_{se}]=\frac{\partial\{P_{se}\}}{\partial\{U_{se}\}}\end{aligned} \tag{45}$$

where $\otimes$ denotes a tensor product, and [I] is the identity matrix of size $N_{DOF} \times N_{DOF}$, where N_{DOF} is the size of the finite element system. The vectors $\{U_{se}\}$, $\{P_{se}\}$, and $\{F_{se}\}$, are a collocation of the deformation, internal, and external forces, respectively, at each nodal time, grouped by common structural degrees of freedom. For example:

$$\{U_{se}\} = \left\{ \begin{Bmatrix} u_1|_{t_1} \\ u_1|_{t_2} \\ \vdots \\ u_1|_{t_{m\times N_{el}}} \end{Bmatrix}^T \quad \cdots \quad \begin{Bmatrix} u_{N_{DOF}}|_{t_1} \\ u_{N_{DOF}}|_{t_2} \\ \vdots \\ u_{N_{DOF}}|_{t_{m\times N_{el}}} \end{Bmatrix}^T \right\}^T \tag{46}$$

Similar quantities are given for the nonlinear internal force and the external force. As above, the solution of this system is facilitated with a nonlinear Jacobian matrix and a residual vector:

$$[J_{se}] = [M] \otimes [\Psi_m] + [C] \otimes [\Psi_c] + [I] \otimes [I_\omega] \cdot [K_{se}] \tag{47}$$

$$\{R_{se}\} = ([M] \otimes [\Psi_m] + [C] \otimes [\Psi_c]) \cdot \{U_{se}\} + [I] \otimes [I_\omega] \cdot (\{P_{se}\} - \mu \cdot \{F_{se}\}) \tag{48}$$

The system can be solved with a Newton-Raphson equilibrium loop, as in Eq. 32.

A sensitivity analysis of the spectral element method proceeds in a very similar manner to the above cyclic-implicit method. The objective function is defined with a quadrature rule:

$$g_{se} = \{\omega\}^T \cdot \{G_{se}\} \qquad \{\omega\} = \mathrm{diag}([I_\omega]) \qquad \{G_{se}\} = \left\{G|_{t_1} \quad G|_{t_2} \quad \cdots \quad G|_{t_{m\times N_{el}}}\right\}^T \tag{49}$$

This system of equations for solution of the adjoint vector is:

$$\{\lambda_{se}\}^T \cdot [J_{se}] = -\{\omega\}^T \cdot \frac{\partial\{G_{se}\}}{\partial\{U_{se}\}} \tag{50}$$

The design sensitivities are given by:

$$\begin{aligned} \left\{\frac{\partial g_{se}}{\partial x}\right\} = \{\lambda_{se}\}^T & \\ \cdot \left(\frac{\partial([M] \otimes [\Psi_m])}{\partial\{x\}} \cdot \{U_{se}\} + \frac{\partial([C] \otimes [\Psi_c])}{\partial\{x\}} \cdot \{U_{se}\} + [I] \otimes [I_\omega] \right. & \\ \left. \cdot \left(\frac{\partial\{P_{se}\}}{\partial\{x\}} - \frac{\partial\{F_{se}\}}{\partial\{x\}} \right) \right) & \end{aligned} \tag{51}$$

As above, the spectral element techniques given in this section can be used for either the full or the reduced order modeling, by substituting the appropriate reduced terms in the various equations.

A comparison between the spectral element method and the cyclic-implicit method is given in Figure 5; the logarithmic error in the objective function and the norm of the gradient vector is plotted as a function of the number of time steps per actuation cycle. The error is given as the difference between the current solution and the solution computed with 600 temporal degrees of freedom. For the spectral element results, the order of the Lagrange basis functions (Eq. 39) is fixed at m = 5; the temporal degrees of freedom are expanded by adding more elements (h-refinement). As would be expected, the higher-ordered spectral elements are more accurate (lower error) than the cyclic-implicit method.

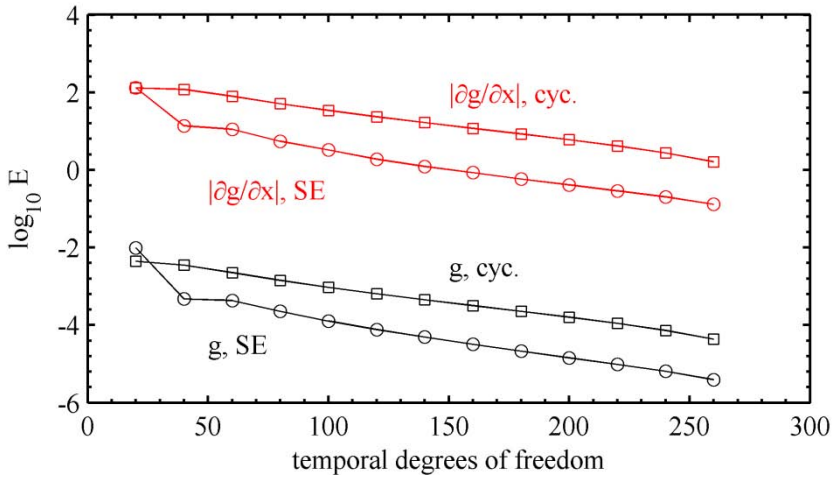

Figure 5. Error metrics, with the polynomial order of the spectral elements (m) fixed at 5: NDOF = 30, ω = 15 rad/s, K = 0.99.

Both time-periodic methods have the option of grouping the solution vector ($\{U_{cyc}\}$ or $\{U_{se}\}$) by common structural degrees of freedom (as formulated for the spectral element method, Eq. 46) or by common temporal degrees of freedom (as formulated for the cyclic-implicit method, Eq. 28). The two choices give drastically different sparsity patterns in the Jacobian matrices, as seen in Figure 6. For the spectral element method, grouping by common structural degree of freedom is preferable, as the matrix is closely banded towards the diagonal. For the cyclic-implicit method, the matrices are twice as large, due to the first order implementation. The method can of course be formulated as a second order system, but this would require a three time level scheme, rather than the two time levels seen in Eq. 27, complicating the process. Grouping by common temporal degree of freedom is slightly superior for the cyclic-implicit method, though neither skyline is very efficient from a sparse-solver standpoint[1].

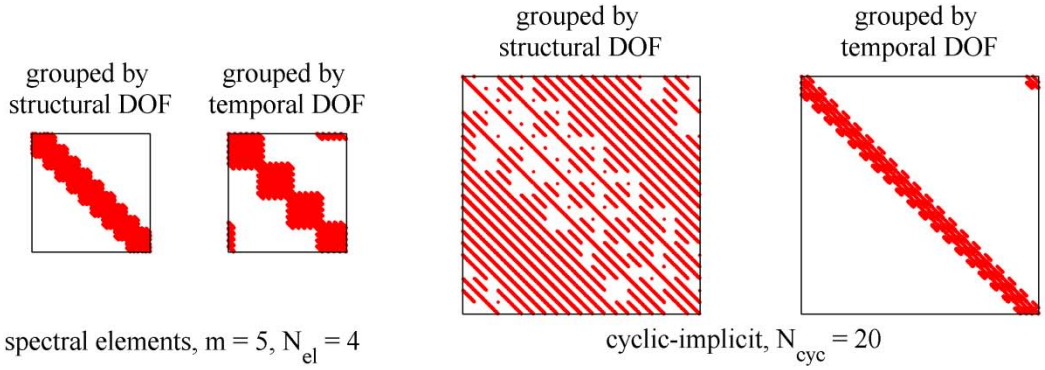

Figure 6. Jacobian sparsity patterns: NDOF = 30, ω = 15 rad/s, K = 0.99.

Neither Figure 5 nor Figure 6 provides an impetus for the use of the cyclic-implicit method over the spectral element method: it isn't as accurate, the Jacobians are twice as large, and the computational effort required for a sparse solver is much higher. As will be seen below, however, the cyclic-implicit method tends to drive the residual of the nonlinear system of equations (Eq. 31) to zero at a faster rate, without relying as heavily upon the load scaling factor. This becomes particularly important for strong nonlinearities, where the spectral element system of equations (Eq. 45) may require the load scaling factor to be slowly increased from 0 to 1 to prevent the system from diverging.

OPTIMIZATION RESULTS

Using the 6 techniques derived above (implicit Newmark time marching, spectral elements, and the cyclic-implicit method, each with or without POD-based model reduction), it is desired to minimize the cycle-integrated tip deflection (Eq. 25), using the cross-sectional area of each beam element as the deign variables {x}. No constraints are considered, other than side constraints. Each element's cross-sectional area is required to be between 2 cm^2 and 6 cm^2. The initial design is a uniform beam with an area of 4 cm^2. Gradient-based optimization is run with a simple steepest-descent algorithm.

For smooth kinematics, decreasing the design parameters {x} will decrease the stiffness of the beam, increasing the deformation. Increasing this variable will increase the weight and thus the inertial loads, also increasing the deformation: an optimal design will utilize a compromise between the two design philosophies. This can be seen in Figure 7, where (for sinusoidal kinematics with K = 0.01) the optimal wing structure is a tapered beam. The beam is very stiff at the root (where the bending moments are largest), and very thin at the tip, where the inertial loads are largest. The side constraints upon the cross-sectional area are enforced at both the root and the tip. Linear and nonlinear deformations require the same beam geometry, as the designs given at 15 and 40 rad/s are identical. These findings are not the case for pseudo-triangular actuation motions (K = 0.99). Deviations from the baseline are relatively small (potentially indicative of a local minimum within the design space), and do not approach the side constraints. Contrasting design philosophies are required for 15 and 40 rad/s, with the former advocating slightly increasing the beam size towards the wing tip.

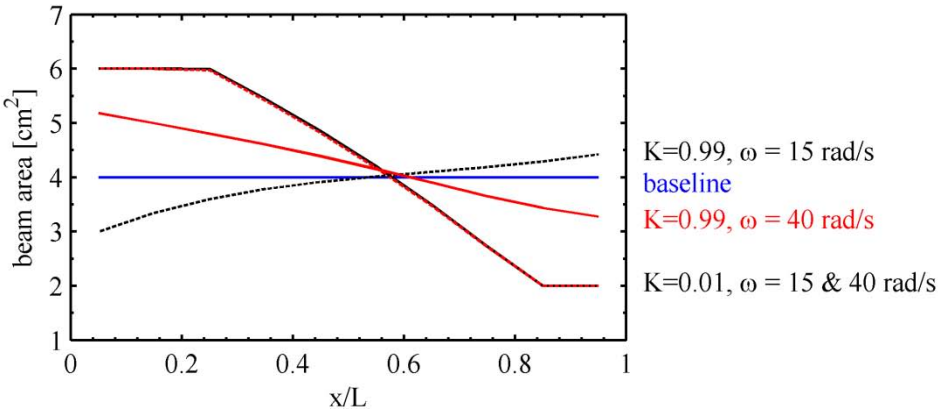

Figure 7. Optimal cross-sectional area distributions for different actuation frequencies and kinematics, with ten finite elements.

The deformation of the beam's tip (δ_{tip}) is given in Figure 8, for a sinusoidal actuation (K = 0.01) at 15 rad/s. Both the transient solution (computed through implicit integration via the Newmark method) and the periodic solution (computed with spectral elements and the cyclic-implicit method, and compared to the last cycle of the Newmark method) are given, computed with the full order model. For the implicit integration, 6 cycles are needed for the deformation to

reach a time-periodic response, and the solution is computed at 100 time steps per cycle. Four spectral elements (N_{el}) are utilized with a 5^{th} order polynomial (m) approximation within each element, while 20 time steps (N_{cyc}) are used for the cyclic-implicit method. It can be seen that the optimal design given in Figure 8 decreases the tip displacement from 4% to 1% of the beam's length. The simple deformation patterns (the natural frequency of the beam itself is evident in the initial transients, but damps out: the remaining response is a sinusoidal trend at the actuation frequency) are well-captured by both time-periodic methods for the baseline and the optimal designs. Only data from the full order models are given in Figure 8: reduced order modeling data should be nearly identical, provided the number of modes and the length of the training period is sufficient (Figure 4).

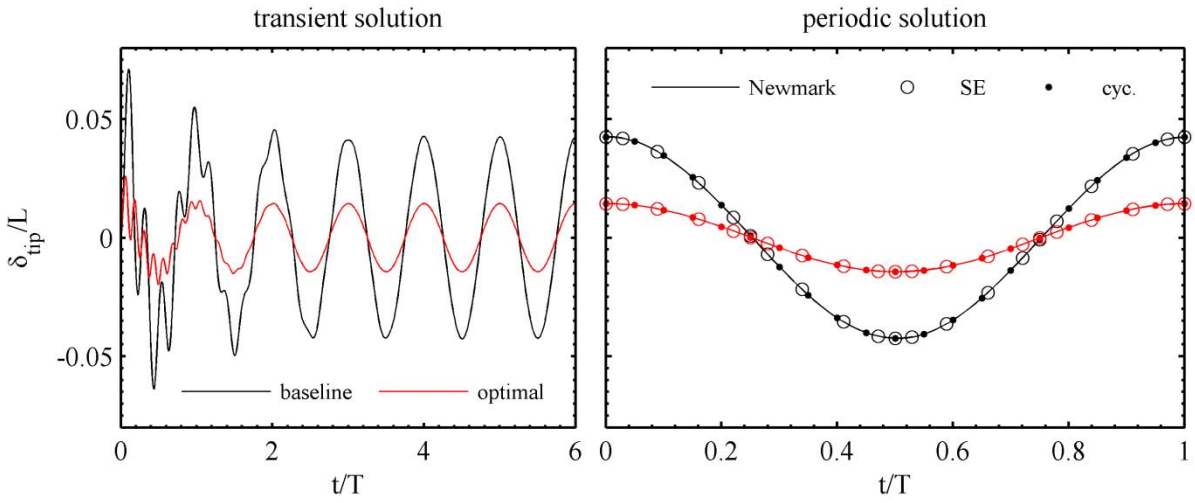

Figure 8. Transient (left) and periodic (right) beam tip deflection for the baseline and optimal designs, computed with the full order model: ω = 15 rad/s, K = 0.01.

The computational cost associated with the optimization of Figure 8 is given in Figure 9, for both 10 and 200 beam elements. Such a fine discretization is not needed for this problem, as both cases give identical results, but the study will give an idea of computational speed-up for future cases with high degrees of freedom. The computational cost of each design iteration is given for all six methods, and includes computer time needed for both the system response computation and the adjoint sensitivities, and in the case of the 3 reduced models, the implicit integration of the full order model through the training period for POD mode computations. For this case, 5 modes were used for 10 beam elements, 7 modes for 200 elements, both with a training period of 0.1·T. All six methods provide nearly-identical responses at each iteration and converge to the same design, though computational effort varies.

The implicit integration of the full order model has the highest cost, while model reduction of the Newmark method provides a speed-up by a factor of 2. Roughly half of this speed-up is due to the reduced cost of the adjoint vector (Eq. 23, where the reduced terms are stored in memory during the forward integration); the remainder is due to reduced solver costs. The relative speed-

up is expected to increase as the size of the full order model (N_{DOF}) increases[17], as well as with higher geometric complexities (with less-favorable sparse skylines than the current case).

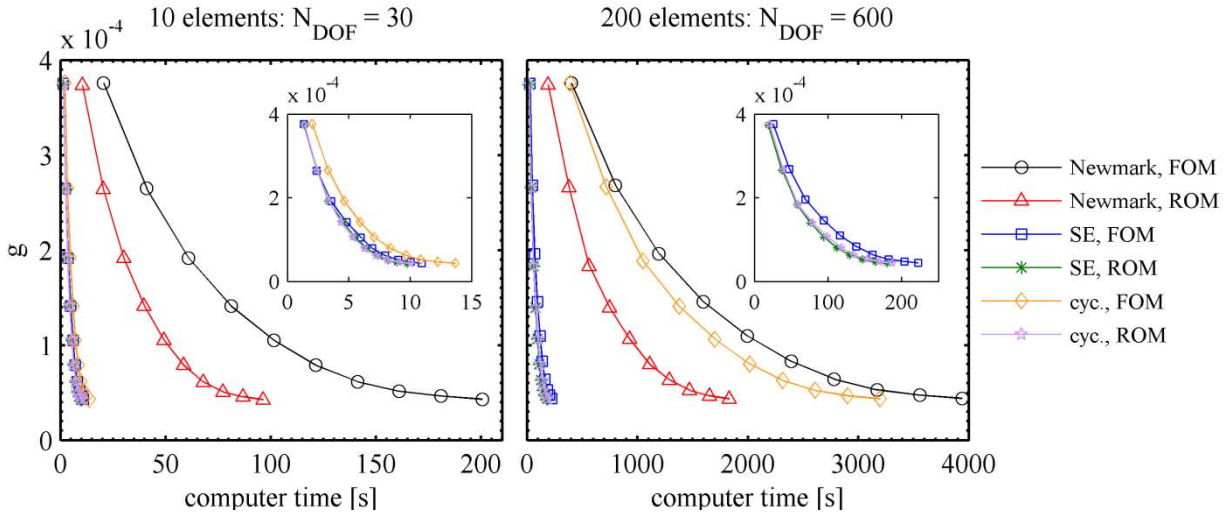

Figure 9. Optimization cost of full and reduced order models: ω = 15 rad/s, K = 0.01.

For this particular case (smooth sinusoidal kinematics with relatively linear structural dynamics), the time-periodic methods are very fast. Convergence of the system is straightforward (the nonlinear systems can be solved directly with μ = 1), and relatively few temporal degrees of freedom are needed. The time-periodic methods provide a speed-up factor of 20, with no significant differences between the spectral element method and the cyclic-implicit method for 10 beam elements. The cost alleviation through model reduction (namely, smaller Jacobians) is offset by the cost of the training period for the POD modes; model reduction of the time-periodic methods has few benefits for this case. Contrastingly, for the larger problem (200 elements) the full order cyclic-implicit method becomes very slow (due to the poor skyline of the Jacobian, Figure 6), and model reduction can be used to drastically decrease the design cost. Increasing the discretization from 10 to 200 elements provides no significant differences in the relative cost associated with the remaining 5 methods.

Similar results are given in Figure 10 and Figure 11, for sinusoidal actuation at 40 rad/s, where the system response of the full order model is reproduced from Figure 3. The higher actuation frequency provides a fairly nonlinear response: the amplitude of the baseline design's deformation is increased from 4% to 40% of the beam's length, though optimization is able to drop the displacement to 10%. Ten actuation cycles are required for the implicit integration to settle within a periodic response, with 200 steps per cycle. As before, the harmonic content of the time-periodic response is low: only 4 spectral elements are needed with a 5^{th} order approximation within each element, while 20 time steps are used for the cyclic-implicit method. Ten POD modes are used to build the reduced models, with a training period of 0.2·T. The relative cost of each method is similar to the previous case, despite the stronger nonlinearities, with the cyclic-implicit method showing a very high cost with finer discretization.

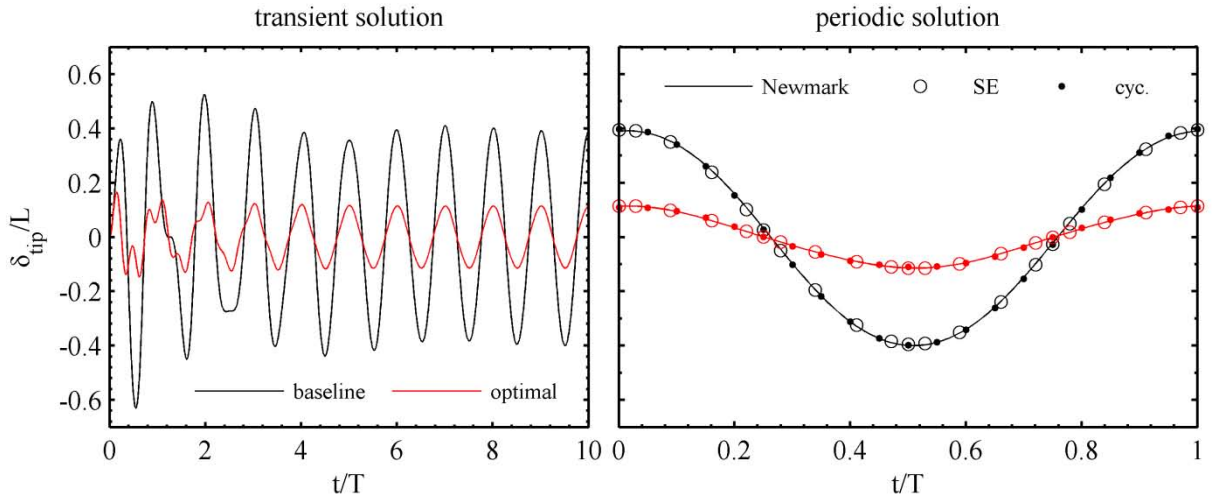

Figure 10. Transient (left) and periodic (right) beam tip deflection for the baseline and optimal designs, computed with the full order model: ω = 40 rad/s, K = 0.01.

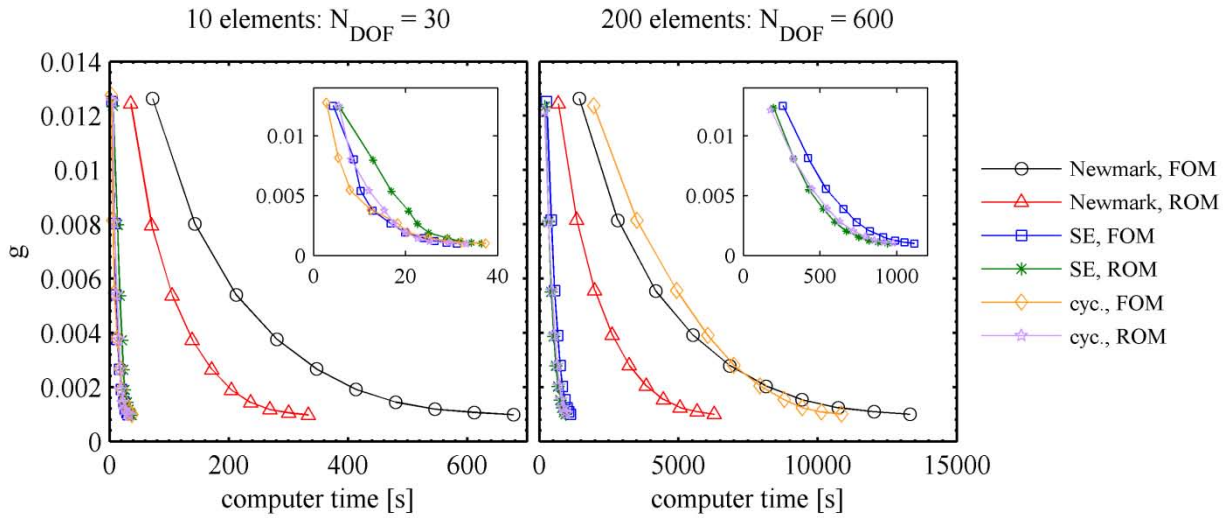

Figure 11. Optimization cost of full and reduced order models: ω = 40 rad/s, K = 0.01.

Results from the pseudo-triangular actuation kinematics (K = 0.99, Figure 2) are given in Figure 12 and Figure 13, for a frequency of 15 rad/s. As expected, a very high harmonic content can be seen in the structural dynamics within each cycle. The inertial forces are essentially zero for the linear portions of the kinematics (seen in Figure 2), while a sudden nonzero acceleration is introduced at the top and bottom of each stroke. For the implicit integration, 6 cycles are needed to reach periodicity, with 300 steps per cycle. For the spectral element method, 25 elements are needed, with a 5th order approximation in each. Presumably, elements could be grouped towards the stroke reversal portions of the actuation for higher accuracy[4], though this is

not done here. For the cyclic-implicit method, 200 time steps are needed during the actuation, nearly twice the temporal degrees of freedom required for the spectral element method, as seen in Figure 5. As above, the time-periodic and the Newmark implicit integration are in close agreement for both the baseline and the optimal designs, both of which show a bi-harmonic response, with the vibration frequency roughly 4 times faster than the actuation frequency.

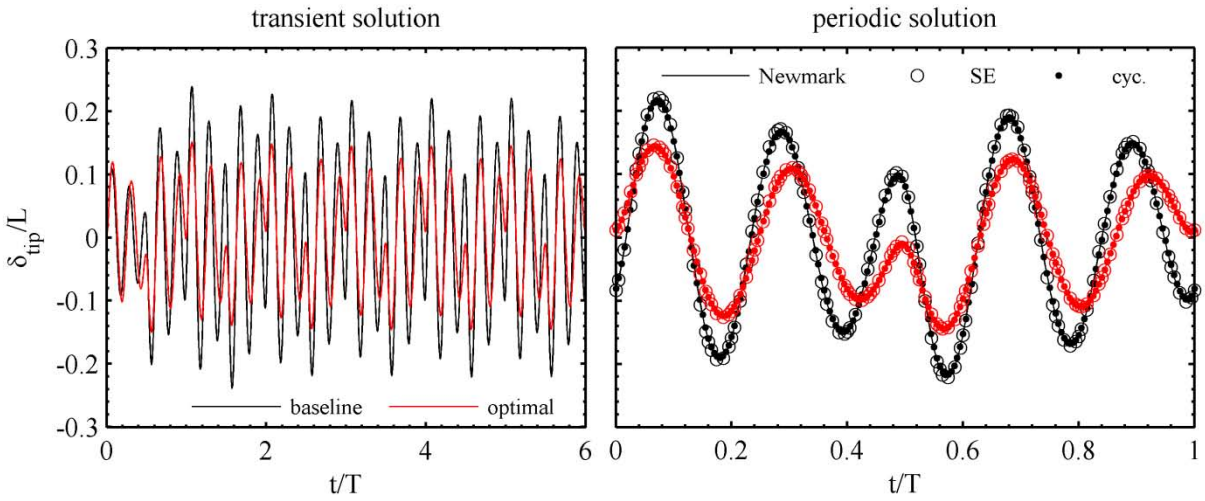

Figure 12. Transient (left) and periodic (right) beam tip deflection for the baseline and optimal designs, computed with the full order model: ω = 15 rad/s, K = 0.99.

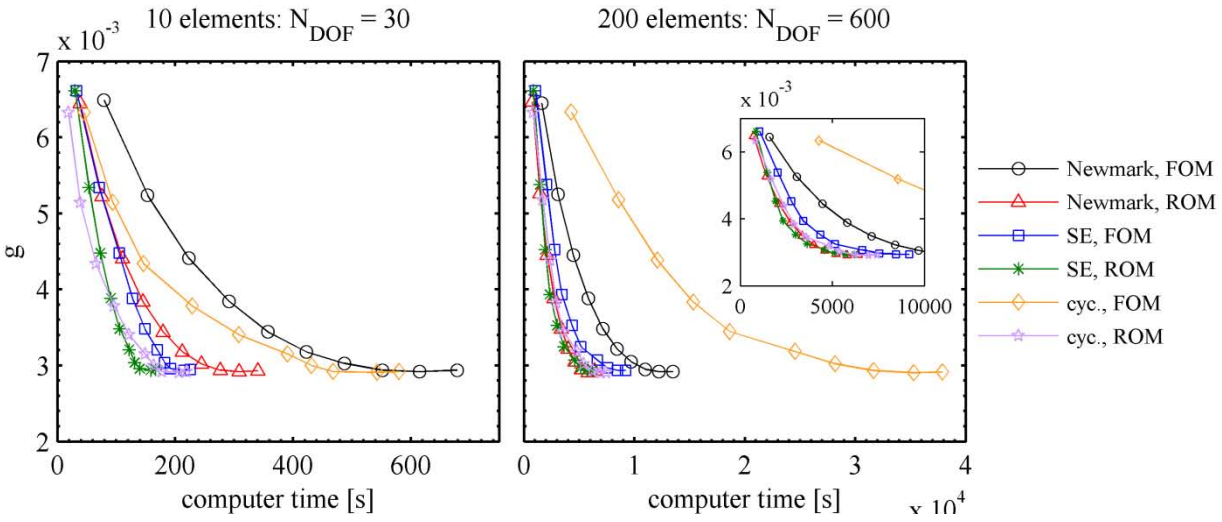

Figure 13. Optimization cost of full and reduced order models: ω = 15 rad/s, K = 0.99.

Computational costs (Figure 13) show a significant redistribution of the run times of the 6 methods (where each ROM uses 6 and 12 POD modes for the coarse and fine discretization,

respectively): specifically, the speed-up of the time-periodic methods becomes less pronounced, as the Jacobians become very large with high temporal degrees of freedom, and system solver costs escalate. The full order cyclic-implicit method becomes very uncompetitive, with a computational cost 3 times higher than the full order Newmark integration. Model reduction can be used to alleviate this cost, of course, with the two reduced time-periodic methods providing the lowest design cost for this case. The speed-up of the reduced spectral element method over the full method is less drastic than seen with the cyclic-implicit method, as the full Jacobians are well-banded (Figure 6).

Finally, results are given in Figure 14 and Figure 15 for an actuation frequency of 40 rad/s and a K of 0.99. The beam vibrates at roughly twice the actuation frequency, with a strongly nonlinear response (40% of the beam length, with the optimal design slightly less, at 30%): this presents a very difficult case for the time-periodic solvers to compute. For the implicit integration, 10 cycles are needed to reach periodicity, with 200 steps per cycle. For the spectral element method, 25 elements are needed with a 5^{th} order approximation in each, while 125 time steps are needed for the cyclic-implicit method. The efficacy of the spectral element method (either full or reduced) suffers for this case, as a fairly low load scaling factor (gradually increased to 1) is needed to prevent the nonlinear system of equations (Eq. 45) from diverging. As noted above, the cyclic-implicit method shows superior convergence characteristics within the Newton-Raphson loop, and has the lowest computational cost of any of the choices in Figure 15 (as long as model reduction is used). It can also be seen than the reduced Newmark integration has relatively low design costs for this case: time-periodic methods become less favorable for structural dynamics cases with high frequency content and strong nonlinearities.

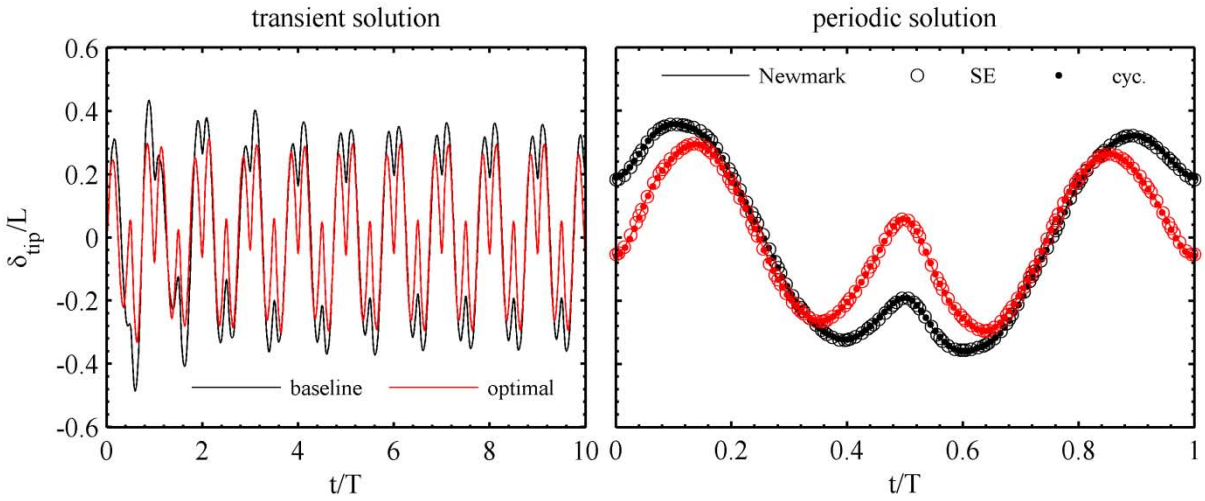

Figure 14. Transient (left) and periodic (right) beam tip deflection for the baseline and optimal designs, computed with the full order model: ω = 40 rad/s, K = 0.99.

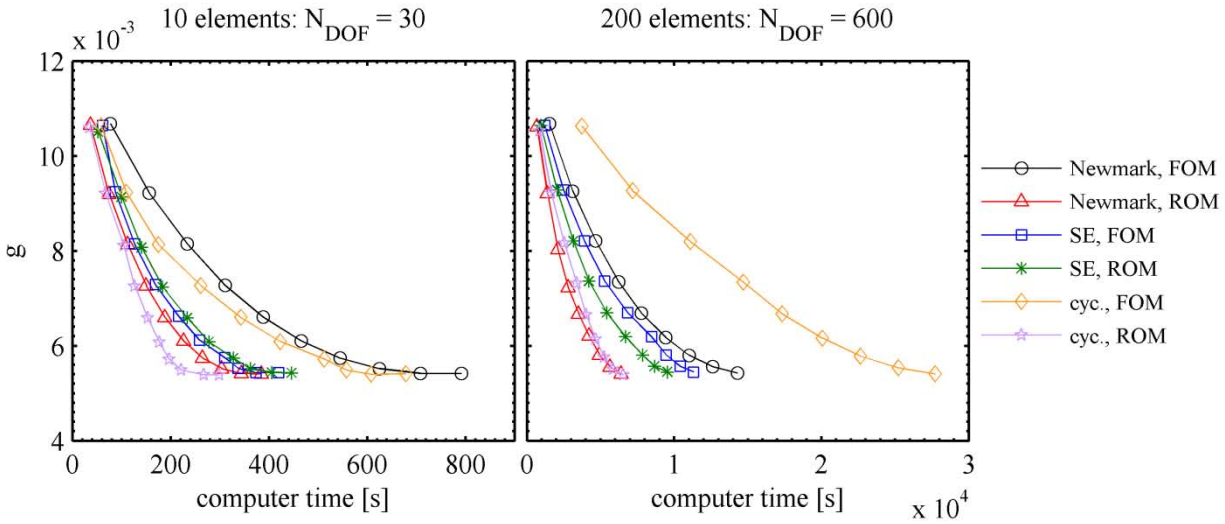

Figure 15. Optimization cost of full and reduced order models: ω = 40 rad/s, K = 0.99.

CONCLUSIONS

This work has detailed efforts intended to reduce the computational cost associated with the gradient-based design of nonlinear rotary beam vibrations. The equations of motions, formulated with a nonlinear corotational method and standard multibody dynamics techniques, are solved with six methods: implicit time marching, a cyclic-implicit method, and a spectral element method, each with or without POD-based model reduction. Upon computation of the system response, gradients of the transient response with respect to a large vector of structural design parameters are computed with the adjoint method, to obtain a computational cost nearly independent of the number of design variables. This information is then used for gradient-based optimization. The following conclusions can be drawn:

1. For implicit integration, the low storage costs associated with model reduction allow for extremely inexpensive reverse integration of the adjoint vector, though more modes are typically needed for an accurate adjoint computation than for the forward integration of the system response. Stability can be a concern during the adjoint computation if the number of modes is insufficient.

2. The addition of more modes to an implicitly integrated reduced order model allows for a shorter training period, to an extent. The number of modes required for a given level of accuracy is a weak function of the number of structural degrees of freedom.

3. The time-periodic spectral element solver is typically more accurate than the cyclic-implicit method for a given number of temporal degrees of freedom, and also has a much more benevolent skyline for solving sparse systems of equations. The latter method, however, has better convergence characteristics within a nonlinear Newton-Raphson loop.

4. Due to unfavorable sparsity patterns, the computational cost of the cyclic-implicit method becomes very large for problems requiring high structural or temporal degrees of freedom; POD-based model reduction can be used to attenuate this cost substantially.

5. Implicit integration with model reduction consistently provides a speed-up factor between 2 and 2.5 over full order time marching for the problem considered here. This number is expected to improve for structures with greater geometric complexity requiring finer meshes.

6. For problems with a low harmonic content (smooth sinusoidal actuation), either time-periodic method, with or without model reduction (with the exception given in point 4), will substantially improve the design cost over time-marching methods.

7. For relatively linear problems with a high harmonic content (i.e., requiring many temporal degrees of freedom), model reduction must be used to limit the computational cost of the time-periodic methods. For stronger nonlinearities, the spectral element method suffers due to convergence problems within the Newton-Raphson loop: the reduced cyclic-implicit method is shown to be superior.

ACKNOWLEDGMENTS

This work is sponsored by the Air Force Office of Scientific Research under Laboratory Task 99VA01COR monitored by Dr. Victor Giurgiutiu, as well as Laboratory Task 09RB01COR monitored by Dr. John Schmisseur. The research was performed while the first and third authors held a National Research Council Associateship Award at AFRL.

REFERENCES

1. Cook, R., Malkus, D., Plesha, M., Witt, R., *Concepts and Applications of Finite Element Analysis*, Wiley, New York, 2002.

2. Belytschko, T., Schoeberle, D., "On the Unconditional Stability of an Implicit Algorithm for Nonlinear Structural Dynamics," *Journal of Applied Mechanics*, Vol. 42, No. 4, pp. 865-869, 1975.

3. Kuhl, D., Crisfield, M., "Energy-Conserving and Decaying Algorithms in Non-Linear Structural Dynamics," *International Journal for Numerical Methods in Engineering*, Vol. 45, No. 5, pp. 569-599, 1999.

4. Kurdi, M., Beran, P., "Spectral Element Method in Time for Rapidly Actuated Systems," *Journal of Computational Physics*, Vol. 227, No. 3, pp. 1809-1835, 2008.

5. van Keulen, F., Haftka, R., Kim, N., "Review of Options for Structural Design Sensitivity Analysis. Part 1: Linear Systems," *Computer Methods in Applied Mechanics and Engineering*, Vol. 194, No. 30, pp. 3213-3243, 2005.

6. Kim, N., Choi, K., "Design Sensitivity Analysis and Optimization of Nonlinear Transient Dynamics," *AIAA Symposium on Multidisciplinary Analysis and Optimization*, Long Beach, CA, September 6-8, 2000.

7. Trier, S., Marthinsen, A., Sivertsen, O., "Design Sensitivities by the Adjoint Variable Method in Nonlinear Structural Dynamics," *SIMS Simulation Conference*, Trondheim, Norway, June 11-13, 1996.

8. Haftka, R., Gürdal, Z., *Elements of Structural Optimization*, Kluwer, The Netherlands, 1992.

9. Kurdi, M. Beran, P., Stanford, B., Snyder, R., "Optimal Actuation of Nonlinear Resonant Systems," *Structural and Multidisciplinary Optimization*, accepted for publication, 2009.

10. Chen, S., Cheung, Y., Xing, H., "Nonlinear Vibration of Plane Structures by Finite Element and Incremental Harmonic Balance Method," *Nonlinear Dynamics*, Vo. 26, No. 1, pp. 87-104, 2001.

11. Liu, L., Thomas, J., Dowell, E., Attar, P., Hall, K., "A Comparison of Classical and High Dimensional Harmonic Balance Approaches or a Duffing Oscillator," *Journal of Computational Physics*, Vol. 215, No. 1, pp. 298-320, 2006.

12. Beran, P., Lucia, D., "A Reduced Order Cyclic Method for Computation of Limit Cycles," *Nonlinear Dynamics*, Vol. 39, No. 1, pp. 143-158, 2005.

13. Kapania, R., Park, S., "Nonlinear Transient Response and its Sensitivity Using Finite Elements in Time," *Computational Mechanics*, Vol. 17, No. 5, pp. 306-317, 1996.

14. Bar-Yoseph, P., Fisher, D., Gottlieb, O., "Spectral Element Methods for Nonlinear Spatio-Temporal Dynamics of an Euler-Bernoulli Beam," *Computational Mechanics*, Vol. 19, No. 2, pp. 136-151, 1996.

15. Gopinath, A., Beran, P., Jameson, A., "Comparative Analysis of Computational Methods for Limit-Cycle Oscillations," *AIAA Structures, Structural Dynamics, and Materials Conference*, Newport, RI, May 1-4, 2006.

16. Lucia, D., Beran, P., Silva, W., "Reduced-Order Modeling: New Approaches for Computational Physics," *Progress in Aerospace Sciences*, Vol. 40, No. 1, pp. 51-117, 2004.

17. Krysl, P., Lall, S., Marsden, J., "Dimensional Model Reduction in Nonlinear Finite Element Dynamics of Solids and Structures," *International Journal for Numerical Methods in Engineering*, Vol. 51, No. 4, pp. 479-504, 2001.

18. Berman, G., Wang, Z., "Energy-Minimizing Kinematics in Hovering Insect Flight," *Journal of Fluid Mechanics*, Vol. 582, pp. 153-168, 2007.

19. Elkaranshawy, H., Dokainish, M., "Corotational Finite Element Analysis of Planar Flexible Multibody Systems," *Computers and Structures*, Vol. 54, No. 5, pp. 881-890, 1995.

20. Kang, B., Park, G., Arora, J., "A Review of Optimization of Structures Subjected to Transient Loads," *Structural and Multidisciplinary Optimization*, Vol. 31, No. 2, pp. 81-95, 2006.

21. Pozrikidis, C., *Introduction to Finite and Spectral Element Methods Using Matlab*, CRC Press, Boca Raton, 2005.

22. Stanford, B., Beran, P., "Cost Reduction Techniques for the Structural Design of Nonlinear Flapping Wings," *AIAA Structures, Structural Dynamics, and Materials Conference*, Palm Springs, CA, May 4-7, 2009.